MID-INFRARED EXTINCTION BY SULFATE AEROSOLS FROM THE MT PINATUBO ERUPTION

C. P. RINSLAND,† G. K. YUE,† M. R. GUNSON,‡ R. ZANDER,§ and M. C. ABRAMS‡

†Atmospheric Sciences Division, NASA Langley Research Center, Hampton, VA 23681-0001, ‡Jet Propulsion Laboratory, California Institute of Technology, Pasadena, CA 91109, U.S.A., and §Institute of Astrophysics, University of Liège, 4000 Liège-Ougreé, Belgium

Abstract—Quantitative measurements of the wavelength dependence of aerosol extinction in the 750–3400 cm^{-1} spectral region have been derived from 0.01 cm^{-1} resolution stratospheric solar occultation spectra recorded by the ATMOS (Atmospheric Trace Molecule Spectroscopy) Fourier transform spectrometer about $9\frac{1}{2}$ months after the Mt Pinatubo volcanic eruption. Strong, broad aerosol features have been identified near 900, 1060, 1190, 1720, and 2900 cm^{-1} below a tangent height of ~ 30 km. Aerosol extinction measurements derived from ~ 0.05 cm^{-1} wide microwindows nearly free of telluric line absorption in the ATMOS spectra are compared with transmission calculations derived from aerosol size distribution profiles retrieved from correlative SAGE (Stratospheric Aerosol and Gas Experiment) II visible and near i.r. extinction measurements, seasonal and zonally averaged H_2SO_4 aerosol weight percentage profiles, and published sulfuric acid optical constants derived from room temperature laboratory measurements. The calculated shapes and positions of the aerosol features are generally consistent with the observations, thereby confirming that the aerosols are predominantly concentrated H_2SO_4–H_2O droplets, but there are significant differences between the measured and calculated wavelength dependences of the aerosol extinction. We attribute these differences as primarily the result of errors in the calculated low temperature H_2SO_4–H_2O optical constants. Errors in both the published room temperature optical constants and the limitations of the Lorentz–Lorenz relation are likely to be important.

1. INTRODUCTION

The eruption of the Mt Pinatubo volcano in the Philippine Islands in June 1991 resulted in the injection of approximately 20 megatons of sulfur dioxide (SO_2), primarily into the stratosphere.[1] The subsequent conversion of the SO_2 into stratospheric sulfate aerosols produced strong extinction which has had a major impact on remote sensing measurements performed in the i.r. and visible spectral regions.[1-6]

Approximately $9\frac{1}{2}$ months after the Mt Pinatubo volcanic eruption, the ATMOS (Atmospheric Trace Molecule Spectroscopy) Fourier transform spectrometer recorded broadband, 0.01 cm^{-1} resolution i.r. solar occultation spectra during the Atmospheric Laboratory for Applications and Science (ATLAS)-1 shuttle mission (24 March to 2 April 1992). The ATMOS stratospheric spectra show strong, broad absorption features attributable to the sulfate aerosols at a higher spectral resolution than that attained in previous post-volcanic i.r. spectroscopic measurements.[6-9] This paper reports initial results obtained from the analysis of the measured i.r. aerosol extinction with emphasis on its dependence with wavenumber.

2. ATMOS/ATLAS 1 OBSERVATIONS

The ATMOS instrument recorded interferograms at 2.2 sec intervals during 53 sunrises between 30°N and 32°S latitude and 41 sunsets between 22°S and 54°S latitude during the ATLAS 1 shuttle mission. From the orbital altitude of ~ 300 km, the time between successive observations corresponded to tangent altitude separations of about 3 km in the upper atmosphere, declining to about 2 km in the lower stratosphere because of refraction and movement of the instrument field of view on the solar disk. One among a series of overlapping, broadband interference filters was

used to limit the spectral coverage during each occultation event. The results reported here were obtained from occultations recorded with filters covering the regions $600-1200\,cm^{-1}$, $600-2500\,cm^{-1}$, or $1580-3400\,cm^{-1}$. Intensities in the individual low sun spectra were ratioed to corresponding values in a mean high sun (exoatmospheric) spectrum derived from observations during the same occultation event. This ratioing procedure removed solar features, lines of H_2O and CO_2 from residual air within the interferometer, and the wavelength dependence of the instrument-filter-detector system response. Detailed information about the ATMOS instrument, its operation and performance, and ATMOS data processing and analysis procedures can be found in Refs. 10–12.

Below a tangent height of 30 km, the Mt Pinatubo aerosols produced significant attenuation throughout the spectral region covered by the ATMOS measurements. For this reason, absolute transmissions could not be determined from the spectra. The ATMOS intensities presented in this paper have been multiplied by a scale factor determined either by normalizing the measured values with respect to the highest intensity in the spectrum or by requiring that the measured intensity at a specific wavelength agree with the transmission calculated for that wavelength from correlative aerosol measurements. As will be shown, these calculated transmittances are subject to considerable uncertainty. Hence, while the wavelength, altitude, and latitude dependences of the aerosol extinction are accurately determined from the ATMOS observations, the absolute transmissions are not.

Figures 1 and 2 illustrate portions of typical mid-stratospheric spectra. The measurements in Fig. 1 were recorded near 54.5°S latitude and 39.6°E longitude on 1 April 1992, during occultation SS47 (SS = sunset). Both spectra in Fig. 1 have been normalized to the highest measured intensity, and the upper spectrum is offset vertically by 0.2 for clarity. Based on spacecraft ephemeris
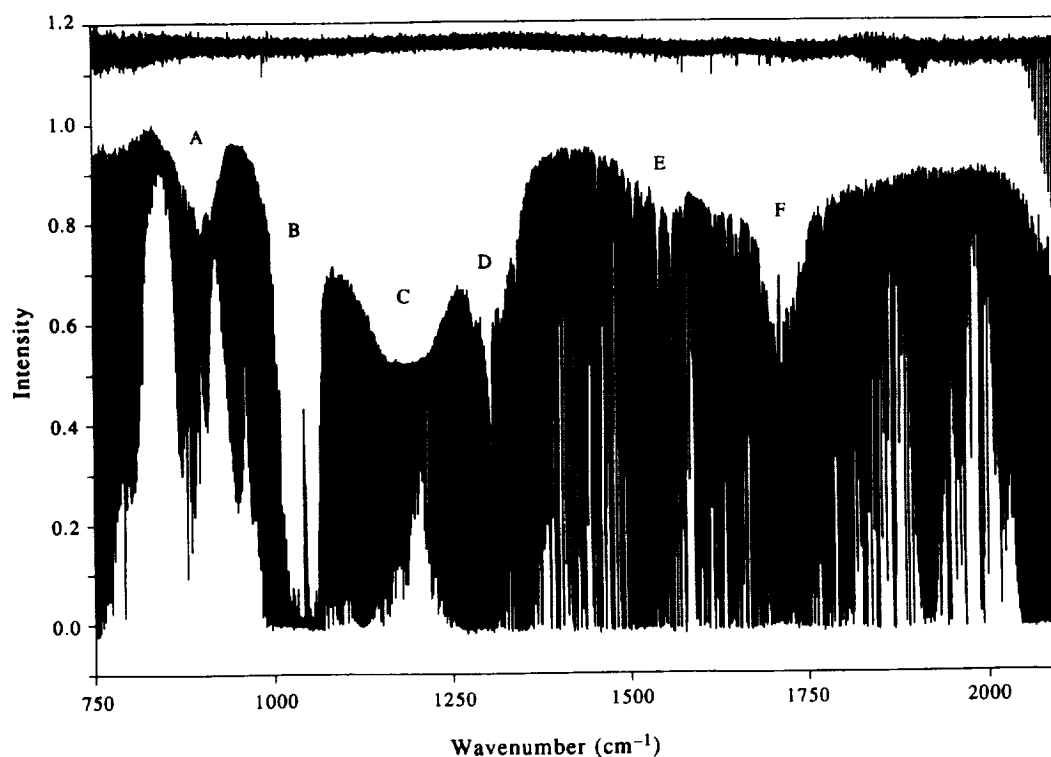

Fig. 1. Portions of solar spectra from sunset occultation SS47 recorded near 54.5°S latitude and 39.6°E longitude, on 1 April 1992, at $14^h\,58^m$ U.T. The spectra are normalized to the highest measured intensity, and the upper scan is offset vertically by 0.2 for clarity. The tangent heights of the upper and lower spectra are 85.9 and 20.9 km, respectively. The pressure and temperature at the tangent altitude of the lower spectrum are 49 mb and 221.2 K, respectively. Prominent molecular absorption and aerosol extinction features are marked in the lower spectrum. See text for the identifications.
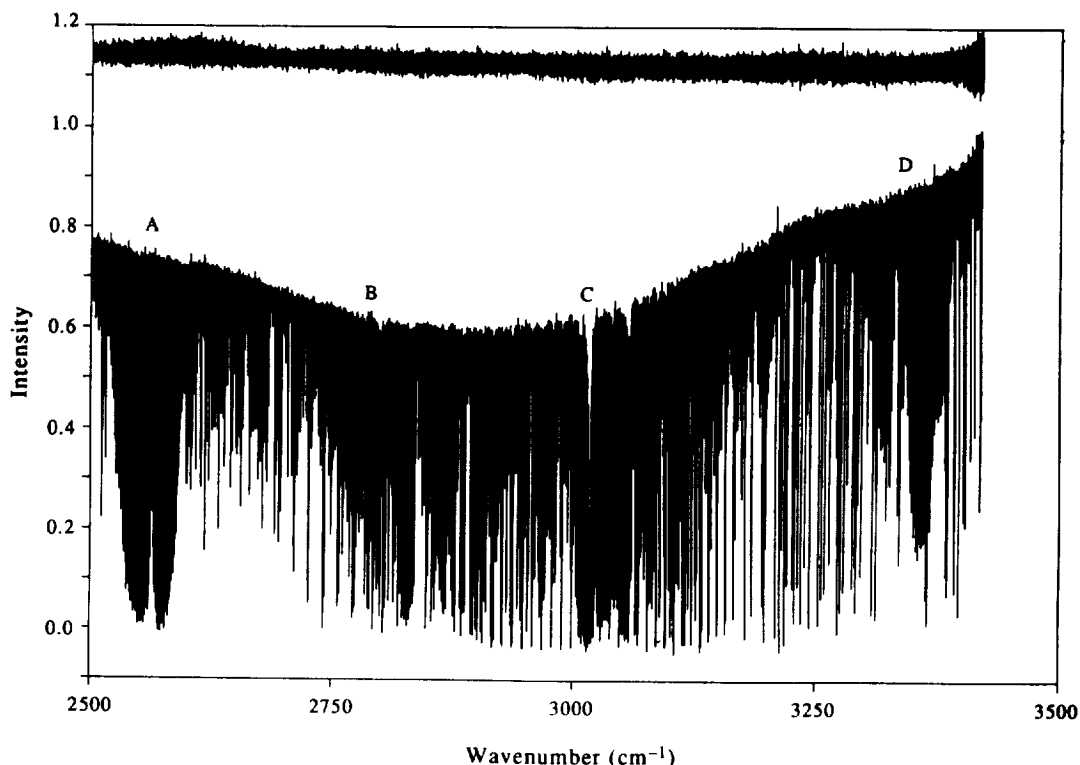
Fig. 2. Portions of solar spectra from sunset occultation SS03 recorded near 22.4°S latitude and 126.4°E longitude on 25 March 1992, at $09^h 37^m$ U.T. The spectra are normalized to the highest measured intensity, and the upper scan is offset vertically by 0.2 for clarity. The tangent heights of the upper and lower spectra are 119.9 and 22.6 km, respectively. The pressure and temperature at the tangent altitude of the lower spectrum are 37.5 mb and 219.8 K, respectively. Prominent molecular absorption and aerosol extinction features are marked in the lower spectrum. See text for the identifications.

information and measurements of CO_2 temperature-independent absorption lines in lower altitude spectra, the tangent height of the upper scan is 85.9 km; the only significant atmospheric absorption features are weak NO lines in the 1800–1900 cm^{-1} region and CO (1–0) band lines above ~2050 cm^{-1}. The lower spectrum was recorded at a tangent height of 20.9 km. This value was derived by least-squares fitting isolated CO_2 temperature-independent absorption lines near 1380 and 1910 cm^{-1} assuming a correlative National Meteorological Center (NMC) pressure-temperature profile[13] and a CO_2 profile with a volume mixing ratio of 3.47×10^{-4} in the lower stratosphere. Six prominent atmospheric absorption features are marked in the lower spectrum: (A) identifies a sulfate aerosol feature at 900 cm^{-1} superimposed on the $2\nu_9$ HNO_3 absorption band; (B) the 1043 cm^{-1} O_3 ν_1 absorption band; (C) a strong, broad sulfate aerosol feature at 1190 cm^{-1}; (D) the ν_4 band of CH_4 at 1307 cm^{-1}; (E) the pressure-induced (1–0) vibration–rotation band of O_2 at 1556 cm^{-1}; and (F) a broad aerosol feature at 1720 cm^{-1} superimposed on HNO_3 and O_3 absorption bands. Spectra recorded during sunrises also show a broad N_2O_5 absorption feature at 1247 cm^{-1}, and the N_2O_5 band at 1716 cm^{-1} adds to the absorption marked F in Fig. 1.

Figure 2 shows a portion of high and low sun spectra from sunset occultation SS03 obtained near 22.4°S latitude and 126.4°E longitude on 25 March 1992. The format of the data is the same as in Fig. 1. The locations and identifications of the most prominent molecular bands in the lower spectrum, obtained at a tangent altitude of 22.6 km, are (A) the $2\nu_1$ band of N_2O at 2563 cm^{-1}, (B) the $\nu_1 + \nu_2 + \nu_3$ band of O_3 at 2785 cm^{-1}, (C) the ν_3 band of CH_4 at 3019 cm^{-1}, and (D) the (21102)–(00001) band of CO_2 at 3339 cm^{-1}. A strong, broad aerosol feature centered near 2900 cm^{-1} absorbs throughout the region. A weaker, narrower aerosol feature is observed near 3350 cm^{-1}.

3. MICROWINDOW MEASUREMENTS

Except in regions of very strong absorption (e.g., in the $1043\,\text{cm}^{-1}$ O_3 band and the $1307\,\text{cm}^{-1}$ v_4 band of CH_4), $\sim 0.05\,\text{cm}^{-1}$ wide "microwindows" nearly free of telluric line absorption have been located throughout the $750–3400\,\text{cm}^{-1}$ region. The measurements in these intervals have been corrected for residual line absorption by dividing the average measured intensity by the average calculated transmission due to molecular lines and the pressure-induced fundamental vibration–rotation band of O_2 ($1425–1736\,\text{cm}^{-1}$ region only). The volume mixing ratio (VMR) profiles adopted in the transmission calculations were retrieved directly from the same spectra for molecules with strong absorption bands, and standard reference profiles (e.g., Ref. 14), updated whenever necessary, were assumed for the molecules with only weak absorption bands. Aerosol extinction does not affect these VMR retrievals because the spectral features are least-squares fitted with respect to the local continuum level, which is well defined at the high resolution of the ATMOS spectra and determined as part of the analysis.

The spectroscopic parameters assumed in our calculations were taken from the ATMOS line parameters compilation,[15] updated for the ATLAS 1 mission according to recent, improved laboratory work. The differences between the updated ATMOS compilation[16] and the 1992 HITRAN compilation[17] are unimportant here except that we simulated the absorption by the O_2 pressure-induced (1–0) band, which is not included in the 1992 HITRAN compilation,[17] with temperature-dependent absorption coefficients.[18] The calculated O_2 absorption we obtain is consistent with the ATMOS measurements from the 1985 Spacelab 3 shuttle mission.[19] The calculations also include the absorption by heavy molecules, such as CCl_2F_2 (CFC-12), CCl_3F (CFC-11), $ClONO_2$, N_2O_5, and CCl_4, computed with the absorption cross sections from the 1992 HITRAN compilation.[17]

Figure 3 illustrates the measurement correction procedure for the spectrum shown in Fig. 1. At top (panel A), the calculated transmittances are plotted; the significant absorptions near 880 and $1570\,\text{cm}^{-1}$ are produced by HNO_3 and O_2, respectively. The middle panel (B) presents the uncorrected ATMOS microwindow measurements; the vertical scale of the data is arbitrary. At bottom (panel C) are the corrected ATMOS measurements, calculated by dividing the uncorrected ATMOS microwindow measurements by the corresponding calculated transmittances. Note that the absorption due to O_2, in particular the Q branch at $1556\,\text{cm}^{-1}$, does not appear in panel C, but the feature near $880\,\text{cm}^{-1}$ remains in panel C, indicating that only part of the measured absorption in that region was produced by HNO_3 lines.

4. WAVELENGTH DEPENDENCE OF THE EXTINCTION

4.1. Transmission Calculations

The wavelength dependence of the extinction has been analyzed by comparing the ATMOS microwindow measurements with sulfate aerosol i.r. transmissions calculated as a function of altitude from correlative SAGE II retrievals of the aerosol size distribution,[20] seasonally and zonally averaged H_2SO_4 aerosol weight percentages determined as a function of latitude and altitude,[21] and the 300 K H_2SO_4–H_2O complex refractive index measurements of Palmer and Williams.[22]

The SAGE II retrieval model[20] assumes that the aerosols have a single mode with a lognormal size distribution. Three parameters, the total number of aerosol particles per unit volume of air, the width of the lognormal distribution, and the mode radius are retrieved as a function of altitude for each SAGE II occultation event from the measured extinctions at 4 visible and near i.r. wavelengths.[20]

The SAGE II aerosol composition calculations[20,21] assume Eq. (8) and coefficients of Gmitro and Vermeulen,[23] which relate the H_2SO_4 weight percentage, the equilibrium H_2O partial pressure, and the temperature. Recently, Zhang et al[24] reported experimental H_2O vapor pressure measurements for supercooled sulfuric acid solutions with H_2SO_4 contents from 20–70 wt %. Under normal stratospheric conditions, that is, when the temperature is above 200 K and the water vapor pressure is less than 20×10^{-4} mm, the calculated H_2SO_4 weight percentages obtained with the Gmitro and
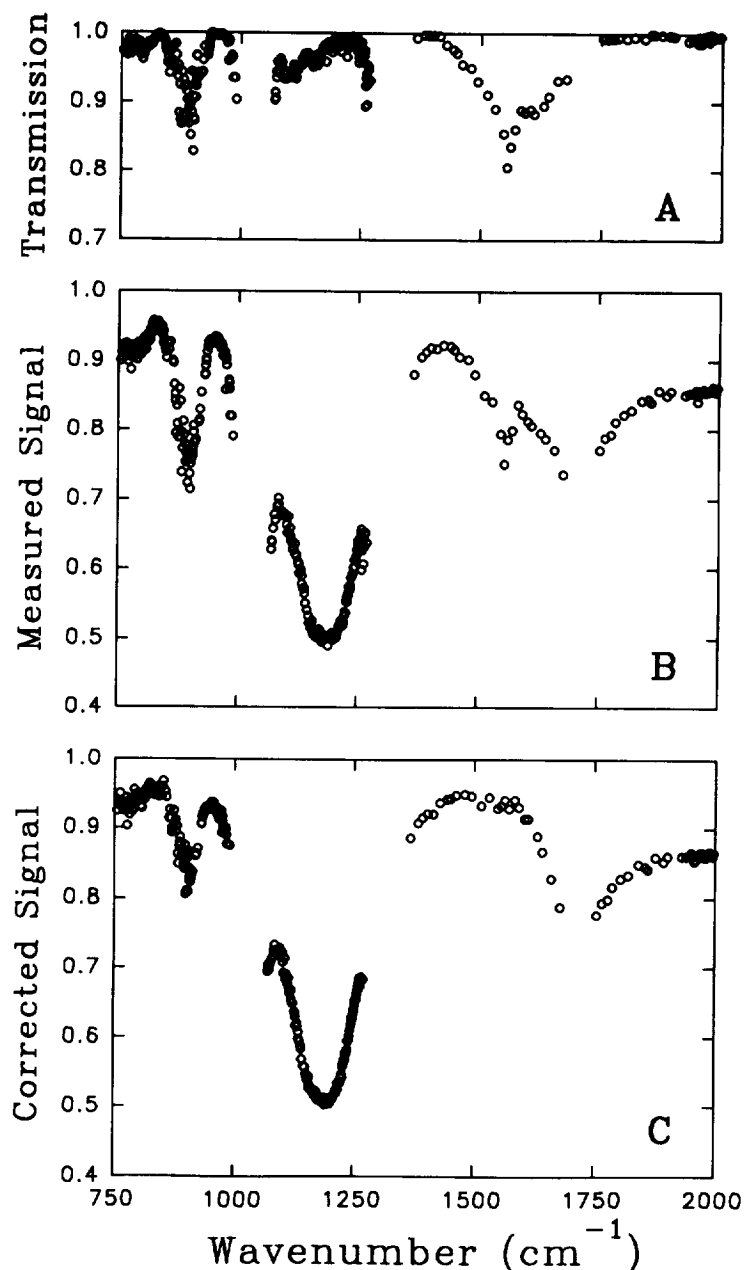
Fig. 3. Example illustrating the procedure used to correct the microwindow measurements for absorption by telluric lines and the O_2 pressure-induced (1-0) band. Panel A: transmissions calculated for the atmospheric path corresponding to the spectrum in Fig. 1. Panel B: uncorrected microwindow measurements derived from the spectrum in Fig. 1. Panel C: corrected microwindow measurements computed by dividing the microwindow measurements in panel B by the calculated transmissions in panel A.

Vermeulen formula and data[23] differ by less than 3% from values computed with Eq. (1) and the coefficients in Table 2 of Zhang et al.[24] Also, under these atmospheric conditions, studies[20,21] have shown that realistic measurement uncertainties in the water vapor partial pressure and the temperature introduce uncertainties of only a few percent in the inferred H_2SO_4 weight percentage. As shown in Fig. 2(b) of Yue et al,[21] the root-mean-square deviation about the zonal and seasonal mean H_2SO_4 weight percentage is 2–3% in the middle stratosphere. We checked the applicability of this climatological acidity dataset[21] by calculating sulfuric acid weight percentage profiles for the occultations included in this investigation assuming the Gmitro and Vermeulen formula and data[23] and the temperatures, pressures, and water vapor mixing ratios retrieved directly from the

ATMOS/ATLAS 1 spectra. A maximum difference of 3% between the individual ATMOS and the SAGE II climatological H_2SO_4 weight percent values[21] was obtained. Based on these investigations, we have assumed a H_2SO_4 weight percent uncertainty of $\pm 5\%$ at all altitudes in the transmission sensitivity calculations which follow.

Palmer and Williams[22] listed experimental 300 K complex refractive index measurements between 400 and 27800 cm^{-1} for aqueous solutions with H_2SO_4 concentrations by weight of 95.6, 84.5, 75, 50, 38, and 25%. We computed optical constants for intermediate concentrations by linear interpolation in these tables. However, as noted by Grainger et al,[4] neither the real (n) or the imaginary (k) part of the refractive index changes monotonically with H_2SO_4 concentration near absorption bands (see Fig. 1 of Ref. 4). We computed the temperature dependence of the $H_2SO_4-H_2O$ refractive index from the Lorentz–Lorenz relation,[25] which is valid far from molecular bands for gases but only an approximation for liquids.[26] Pinkley and Williams[27] interpreted their i.r. measurements of $H_2SO_4-H_2O$ solutions at 250 and 300 K as indicating that the Lorentz–Lorenz equation is valid in spectral regions remote from absorption bands, but their measurements near strong bands showed that it failed.

4.2. Measurement-calculation comparisons

Figure 4 presents a comparison of the ATMOS microwindow measurements from the lower sun spectrum of Fig. 1 with the corresponding calculated transmissions. The measured ATMOS intensities (open circles) have been converted to transmissions by multiplying them by the single
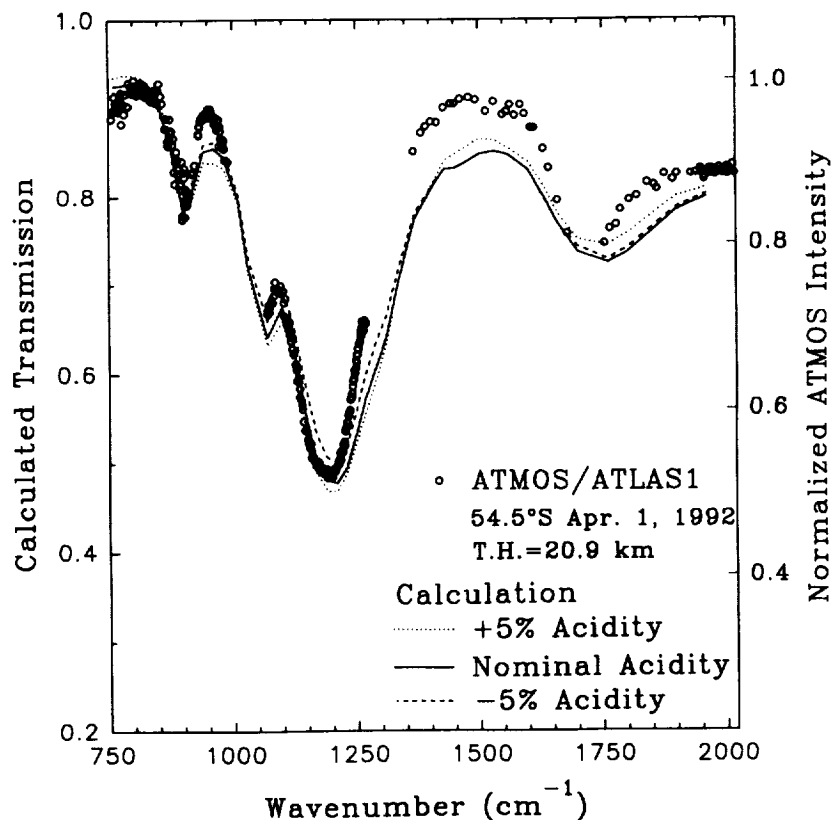

Fig. 4. ATMOS aerosol extinction measurements from the lower sun spectrum of Fig. 1 and calculated transmissions derived from SAGE II aerosol composition climatology,[21] SAGE II aerosol extinction measurements on 4–19 April 1992, at 50°S–60°S, and the Palmer and Williams[22] $H_2SO_4-H_2O$ optical constants. The ATMOS measurements have been scaled vertically by a single multiplicative factor to agree with the calculated transmission at 820 cm^{-1}; the right vertical axis shows the ATMOS intensity scale, normalized with respect to the highest value in the bandpass (600–2500 cm^{-1}). Dashed and dotted lines are calculated transmissions computed with H_2SO_4 weight percentage offsets at all altitudes of $+5$ and -5%, respectively.

scale factor that produces agreement with the calculated transmission curve (solid line) at 820 cm^{-1}, where the aerosol extinction is the lowest. The main source of uncertainty in the ATMOS transmissions is this scale factor. As can be seen from the figure, significantly different transmissions would result if another spectral region was selected for determining the scale factor. The precision of the ATMOS measurements, about $\pm 2\%$ (1σ) relative to the peak measured intensity, is limited primarily by the nonlinear response of the HgCdTe detector. This effect introduces zero level offsets and low frequency variations in the measured intensities as can be observed in the upper spectrum of Fig. 1. Additional sources of error in the ATMOS transmissions are the finite signal-to-noise ratio of the measured spectra and errors in the calculated corrections for residual molecular line and O_2 band absorption.

The solid curve in Fig. 4 shows the aerosol transmissions calculated for the tangent altitude of the ATMOS observations. All of the aerosol bands observed in the ATMOS spectrum appear in the calculated spectrum including the 1060 cm^{-1} band which is partially obscured by strong O_3 absorption in the observations. However, the strongest band is narrower in the ATMOS data than in the calculated spectrum, and the location of its maximum absorption is shifted from 1190 ± 1 cm^{-1} in the ATMOS measurements to 1202 cm^{-1} in the calculations. Because of overlapping molecular line absorption, the location of the absorption maximum of the 1700 cm^{-1} band cannot be accurately determined from the ATMOS measurements, but it is clear from the figure that this band also has a different shape and its maximum absorption is shifted to a lower wavenumber as compared to the calculations. Additionally, we note from Fig. 4 that there is poor agreement between the measurements and calculations between 1350 and 1600 cm^{-1}, where aerosol extinction is relatively small. The dashed and dotted curves in Fig. 4 show transmission calculations performed with aerosol acidity offsets at all altitudes of $+5$ and -5%, respectively. The modest changes in the calculated transmissions obtained with these offsets are insufficient to produce agreement with the ATMOS measurements. Several other comparisons between ATMOS data and calculated transmissions have been performed with the characteristic differences noted above found in all cases.

Figure 5 presents a comparison of microwindow measurements from the lower spectrum of Fig. 2 with aerosol transmission calculations for the corresponding conditions. The ATMOS intensity measurements have been scaled by a single multiplicative factor to agree with the calculated transmission at 3180 cm^{-1} where the three calculated curves cross. Maximum aerosol extinction occurs in the ATMOS spectrum at 2883 ± 4 cm^{-1} as compared with 2982 cm^{-1} in the transmission spectrum computed for the nominal H_2SO_4 weight percentage profile. As in Fig. 4, the changes in the calculated transmissions obtained with the $\pm 5\%$ acidity offsets are insufficient to produce agreement with the ATMOS measurements.

4.3. Discussion

The mid-i.r. H_2SO_4-H_2O optical constants of Palmer and Williams[22] have a quoted fractional uncertainty of ± 0.01 for the real component and an uncertainty of ± 0.03 for the imaginary component over most of the measurement range. The authors state that the uncertainty in the components is larger at low frequencies because of increasing uncertainty in the measured reflectance and the influence of the extrapolation of the reflectance below the measurement limit of 350 cm^{-1} on their results.

Remsberg[28] and Remsberg et al[29] measured room temperature optical constants for 75 and 90% aqueous H_2SO_4 solutions at selected wavenumbers between about 748 and 1570 cm^{-1}. As shown in Fig. 11 of the paper by Palmer and Williams,[22] the 75% H_2SO_4 optical constants of Remsberg[28] agree with the corresponding Palmer and Williams[22] optical constants to about the quoted uncertainties except below 1000 cm^{-1} where the difference in the imaginary component is significant and increases with decreasing wavenumber. At 820 cm^{-1}, for example, where the imaginary component is small but important, the Remsberg et al[29] value of k is 1.56 times the corresponding Palmer and Williams[22] value.

To illustrate the effect of the differences in the two sets of optical constants on the transmission calculations, we used the values tabulated by Remsberg et al[29] for 75 and 90% aqueous H_2SO_4 solutions to compute transmissions for the atmospheric path corresponding to the ATMOS observations shown in Fig. 1 (lower spectrum) and Fig. 4. In Fig. 6, the calculated values (dashed
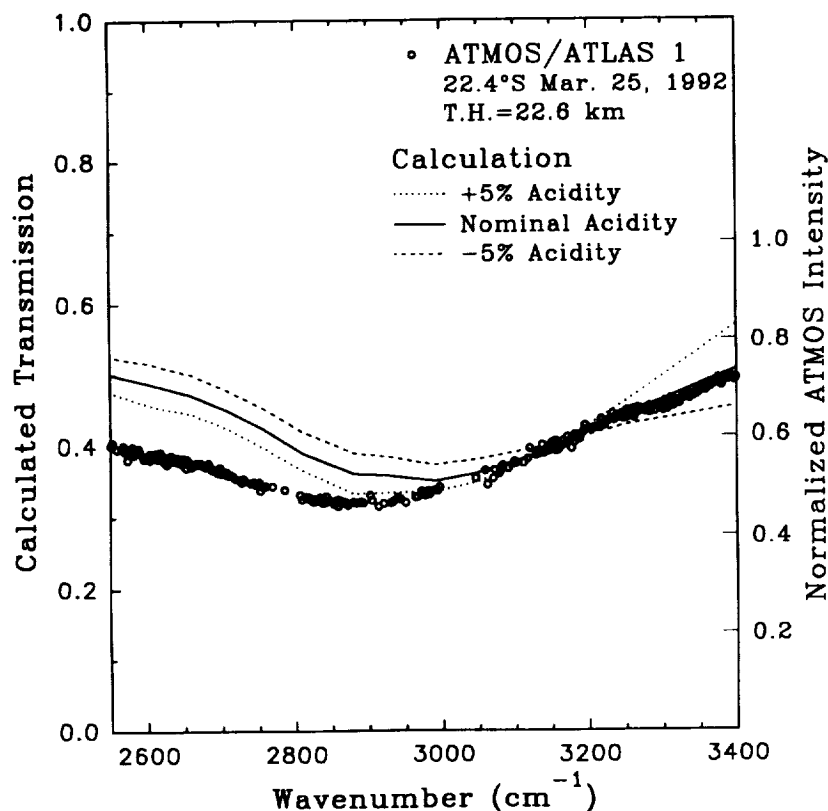
Fig. 5. Aerosol extinction measurements deduced from the lower sun spectrum of Fig. 2 and calculated transmissions derived from SAGE II aerosol composition climatology,[21] SAGE II aerosol extinction measurements on 11 and 12 March 1992, and 27 and 28 March 1992, at 20–25°S latitude, and the Palmer and Williams[22] H_2SO_4-H_2O optical constants. The ATMOS measurements have been scaled vertically by a multiplicative factor to agree with the calculated transmission at 3150 cm^{-1}; the right vertical axis shows the ATMOS intensity scale, normalized with respect to the highest value in the bandpass (1580–3400 cm^{-1}). Dashed and dotted lines are calculated transmissions computed with H_2SO_4-H_2O weight percentage offsets at all altitudes of +5 and −5%, respectively.

line) are presented along with the calculated transmissions obtained with the Palmer and Williams optical constants[22] (solid line, repeated from Fig. 4). Below 1000 cm^{-1} the attenuation calculated with the Remsberg et al[29] optical constants is significantly larger than that calculated with the Palmer and Williams[22] optical constants. In Fig. 6, we included the ATMOS microwindow measurements (open circles) shown in Fig. 4, but with the vertical scaling modified to produce agreement with the calculated 820 cm^{-1} transmission obtained with the Remsberg et al[29] optical constants. Examining Figs. 4 and 6, we find that the Remsberg et al[29] optical constants are in better agreement with the ATMOS measurements than are the transmittances calculated with the Palmer and Williams[22] optical constants. However, neither set of calculated transmissions agree with the ATMOS observations at all wavelengths. Greater precision is generally attributed to results obtained with the technique of attenuated total reflection (ATR) spectroscopy used by Remsberg et al[29] than to results based on liquid surface reflectance measurements, such as those recorded and analyzed by Palmer and Williams.[22]

The effect of temperature on the optical constants of aqueous H_2SO_4 solutions was first investigated by Pinkley and Williams.[27] Based on reflection measurements covering the 400–6000 cm^{-1} region at 250 and 300 K, these authors inferred slight shifts in frequency and significant differences in the imaginary index of refraction at the band maxima for a 75% H_2SO_4 aqueous solution. More recently, Middlebrook et al[30] and Zhang et al[24] reported Fourier transform spectra of liquid and supercooled liquid H_2SO_4-H_2O solutions at temperatures of about 200 K and room temperature. The spectra, which cover 500–4000 cm^{-1}, show large changes in the absorbance with temperature for dilute H_2SO_4 solutions, but the concentrated solutions show only minor
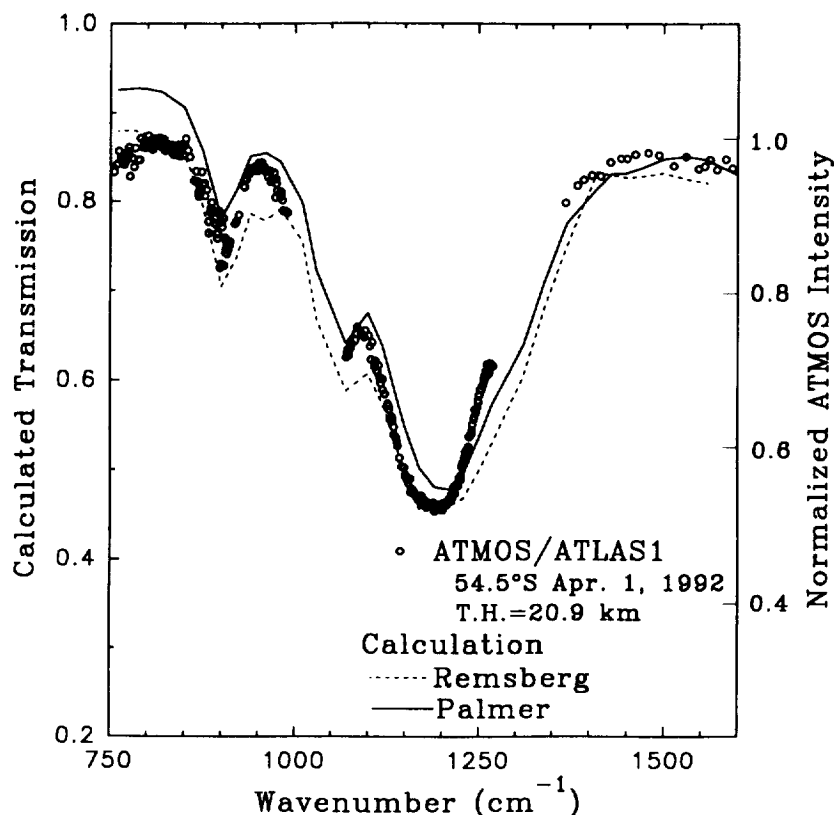
Fig. 6. Aerosol extinction measurements from the lower sun spectrum of Fig. 1 and calculated transmissions derived from SAGE II aerosol composition climatology.[21] SAGE II aerosol extinction measurements on 4–19 April 1992, at 50–60°S, and the Palmer and Williams[22] (solid curve) or the Remsberg et al[29] (dashed curve) H_2SO_4-H_2O optical constants. Only the transmission calculation results derived assuming the nominal (climatological) aerosol acidity profile are plotted for clarity. The ATMOS measurements (open circles) have been scaled vertically by a multiplicative factor to agree with the calculated 820 cm^{-1} transmission obtained with the Remsberg et al[29] H_2SO_4 optical constants; the right vertical axis shows the ATMOS intensity scale, normalized with respect to the highest value in the bandpass (600–2500 cm^{-1}). Note that the vertical scaling of the ATMOS measurements is different in Fig. 6 than in Fig. 4.

changes in the spectral features with cooling. Unfortunately, the plots provided in these papers are insufficient to generate quantitative comparisons with the ATMOS spectra.

The single mode lognormal size distribution assumed in this work and several earlier studies[31,32] of the SAGE II aerosol extinction measurements yields reliable size distribution retrievals when only one lognormal mode is dominant, as is the case under background aerosol conditions, but it produces less satisfactorily results when several modes are present or the size distribution is not lognormal.[20] Although the presence of three aerosol modes was inferred from SAGE II aerosol measurements obtained during the first several months following the Mt Pinatubo volcanic eruption,[33] multimodal size distributions cannot be retrieved from the SAGE II four-channel data. Under such circumstances, the single lognormal size distribution model assumed here produces an effective size distribution with an abnormally large retrieved width. As the aerosol transmission calculations presented in Figs. 4–6 result from size distributions with effective lognormal widths only ∼20% larger than widths inferred from pre-eruption SAGE II measurements near the same latitude, we conclude that a strong secondary mode was not present at those times and locations. Furthermore, as shown by previous studies,[4,8] the calculated wavelength dependence of the extinction in the mid-i.r. is only weakly dependent on the assumed particle size distribution.[4,8] This follows from the fact that the radii of most particles are small compared to the wavelength, and the Rayleigh limit of the Mie theory can be used as an approximation.[8]

5. LATITUDE AND ALTITUDE DEPENDENCE OF THE EXTINCTION

Figure 7 presents a plot of the aerosol extinction index A vs tangent altitude where A is given by

$$A = 1 - I(1184)/I(818)$$

and $I(1184)$ is the intensity at $1184\,\mathrm{cm}^{-1}$ (where aerosol extinction is close to a maximum) and $I(818)$ is the intensity at $818\,\mathrm{cm}^{-1}$ (where aerosol extinction is near a minimum). Data for only two latitude bands (0–10°N and 50–60°S) are plotted for clarity. We note from Fig. 7 that aerosol extinction was detected to an altitude of $\sim 35\,\mathrm{km}$ in the tropics and to $\sim 32\,\mathrm{km}$ at the higher (southern hemisphere) latitudes. The large difference in the aerosol loading in the two latitude bands is apparent. The calculated indices shown in the figure were derived from aerosol size distributions derived from correlative SAGE II aerosol measurements and climatological H_2SO_4 weight percentage profiles,[21] as described in the previous section. The agreement between the measurements and calculations is excellent at low latitudes, but the calculated extinction index is up to a factor of 2 higher than the measured ATMOS value in the high latitude band. As there are only small differences among the individual SAGE II 50°S–60°S measurements (60 profiles between 1 and 4 March 1992, and 216 profiles between 4 and 19 April 1992), the cause of this discrepancy has not been resolved.

In an earlier work,[19] we reported aerosol indices computed from microwindow measurements on ATMOS/Spacelab 3 spectra recorded near 30°N and 47°S latitude in May 1985. The results showed detectable extinction by post-El Chichón eruption aerosols at tangent altitudes between about 15 and 30 km (see Fig. 11 of Ref. 19).
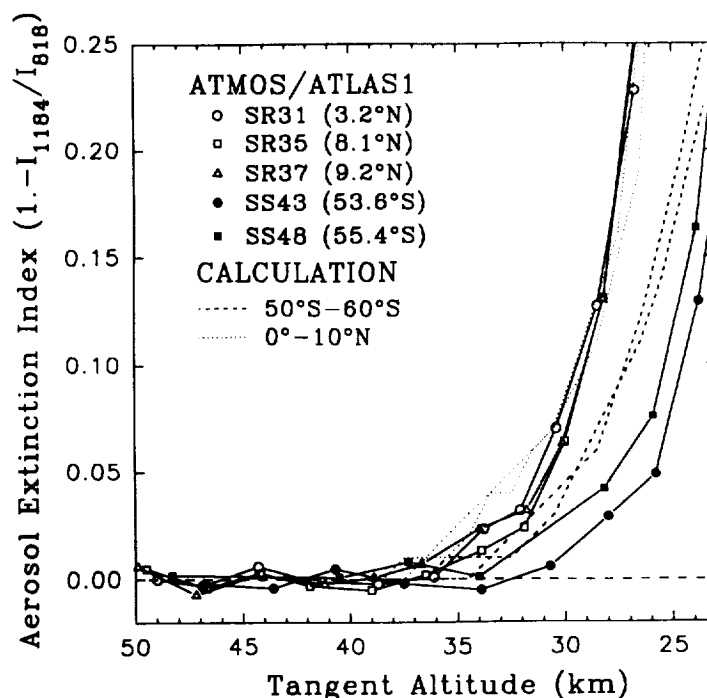

Fig. 7. Aerosol extinction index, defined as one minus the ratio of the intensity at $1184\,\mathrm{cm}^{-1}$ to the intensity at $818\,\mathrm{cm}^{-1}$, plotted vs tangent altitude. ATMOS/ATLAS 1 measurements from two latitude bands are shown along with calculated values derived from the Palmer and Williams optical constants,[22] climatological H_2SO_4 aerosol acidity profiles,[21] and SAGE II aerosol size distribution profiles obtained between 0° to 10°N and 50°S to 60°S. Two calculated curves are plotted for each latitude band: the higher extinction curve is calculated from the average of measurements obtained in March 1992 and the lower extinction curve is calculated from the average of measurements obtained in April 1992. The ATMOS data were measured from spectra recorded during occultations recorded with a filter covering 600–1200 cm⁻¹; estimated precisions and absolute accuracies of the ATMOS index measurements are 0.5 and 1%, respectively.

6. SUMMARY AND CONCLUSIONS

Mid-i.r. stratospheric solar occultation spectra recorded at 0.01 cm^{-1} resolution by the ATMOS Fourier transform spectrometer in late March and early April 1992 have been analyzed with emphasis on the wavelength dependence of the strong post-Mt Pinatubo eruption aerosol extinction. Broad aerosol features with maximum absorptions near 900, 1060, 1190, 1720, and 2900 cm^{-1} have been identified in the spectra. The measured wavelength, altitude, and latitude dependences of the aerosol extinction have been compared with calculated values derived from room temperature H_2SO_4–H_2O optical constants (Ref. 22 or Ref. 29), correlative SAGE II visible and near i.r. measurements of the aerosol size distribution, and climatological sulfate aerosol acidity profiles.[21] Our main finding is that the shapes and the positions of the measured aerosol features are generally consistent with our calculations, thereby confirming studies that show the Mt Pinatubo aerosols are predominantly concentrated sulfuric acid/aqueous droplets.[34,35] However, we find significant differences between the measured and calculated wavelength dependences of the aerosol i.r. extinction. These discrepancies result mostly from errors in the low temperature H_2SO_4–H_2O optical constants, which we had to compute from the room temperature values[22,29] and the Lorentz–Lorenz relation.[25] The failure of these calculations to reproduce the high quality ATMOS measurements shows the need for i.r. laboratory measurements of H_2SO_4–H_2O optical constants as a function of temperature, wavelength, and acidity.

REFERENCES

1. G. J. S. Bluth, S. D. Doiron, C. C. Schnetzler, A. J. Krueger, and L. S. Walter, *Geophys. Res. Lett.* **19**, 151 (1992).
2. L. L. Stowe, R. M. Carey, and P. P. Pellegrino, *Geophys. Res. Lett.* **19**, 159 (1992).
3. M. P. McCormick and R. E. Veiga, *Geophys. Res. Lett.* **19**, 155 (1992).
4. R. G. Grainger, A. Lambert, F. W. Taylor, J. J. Remedios, C. D. Rodgers, M. Corney, and B. J. Kerridge, *Geophys. Res. Lett.* **20**, 1283 (1993).
5. M. E. Hervig, J. M. Russell III, L. L. Gordley, J. H. Park, and S. R. Drayson, *Geophys. Res. Lett.* **20**, 1291 (1993).
6. J. L. Mergenthaler, J. B. Kumer, and A. E. Roche, *Geophys. Res. Lett.* **20**, 1295 (1993).
7. F. C. Witteborn, K. O'Brien, H. W. Crean, J. B. Pollack, and K. H. Bilski, *Geophys. Res. Lett.* **10**, 1009 (1983).
8. B. Halperin and D. G. Murcray, *Appl. Opt.* **26**, 2222 (1987).
9. J. B. Pollack, F. C. Witteborn, K. O'Brien, and B. Flynn, *J. geophys. Res.* **96**, 3115 (1991).
10. C. B. Farmer, *Mikrochem. Acta* **III**, 189 (1987).
11. C. B. Farmer, O. F. Raper, and F. G. O'Callaghan, "Final report on the first flight of the ATMOS instrument during the Spacelab 3 mission, April 29 through May 6, 1985", *JPL Publ. 87-32*, 45 pp., Jet Propulsion Laboratory, Pasadena, California (1987).
12. R. H. Norton and C. P. Rinsland, *Appl. Opt.* **30**, 389 (1991).
13. M. Gelman, National Meteorological Center, private communication (1992).
14. M. A. H. Smith, "Compilation of Atmospheric Gas Concentration Profiles from 0 to 50 km", *NASA Technical Memorandum 83289*, NASA Langley Research Center, Hampton, VA (1982).
15. L. R. Brown, C. B. Farmer, C. P. Rinsland, and R. A. Toth, *Appl. Opt.* **26**, 5154 (1987).
16. L. R. Brown, private communication (1993).
17. L. S. Rothman, R. R. Gamache, R. H. Tipping, C. P. Rinsland, M. A. H. Smith, D. C. Benner, V. Malathy Devi, J.-M. Flaud, C. Camy-Peyret, A. Perrin, A. Goldman, S. T. Massie, L. R. Brown, and R. A. Toth, *JQSRT* **48**, 469 (1992).
18. J. J. Orlando, G. S. Tyndall, K. E. Nickerson, and J. G. Calvert, *J. geophys. Res.* **96**, 20755 (1991).
19. C. P. Rinsland, R. Zander, J. S. Namkung, C. B. Farmer, and R. H. Norton, *J. geophys. Res.* **94**, 16303 (1989).
20. G. K. Yue, M. P. McCormick, and W. P. Chu, *J. Atmos. Ocean. Technol.* **3**, 371 (1986).
21. G. K. Yue, L. R. Poole, P.-H. Wang, and E. W. Chiou, *J. geophys. Res.* **99**, 3727 (1994).
22. K. F. Palmer and D. Williams, *Appl. Opt.* **14**, 208 (1975).

23. J. I. Gmitro and T. Vermeulen, *A.I.C.E. Jl* **10**, 740 (1964).
24. R. Zhang, P. J. Wooldridge, J. P. D. Abbatt, and M. J. Molina, *J. phys. Chem.* **97**, 7351 (1993).
25. R. S. Longhurst, *Geometrical and Physical Optics*, 3rd edn., Chap. 20, p. 506, Longman, New York, NY (1973).
26. J. D. Jackson, *Classical Electrodynamics*, 2nd edn., Chap. 4, p. 155, Wiley, New York, NY (1975).
27. L. W. Pinkley and D. Williams, *J. opt. Soc. Am.* **66**, 122 (1976).
28. E. E. Remsberg, Ph.D. dissertation, Univ. Wisconsin (1971).
29. E. E. Remsberg, D. Lavery, and B. Crawford Jr., *J. chem. Engng Data* **19**, 263 (1974).
30. A. M. Middlebrook, L. T. Iraci, L. S. McNeill, B. G. Koehler, M. A. Wilson, O. W. Saastad, M. A. Tolbert, and D. R. Hanson, *J. geophys. Res.* **98**, 20473 (1993).
31. C. Brogniez, and J. Lenoble, *J. geophys. Res.* **96**, 15479 (1991).
32. P.-H. Wang, M. P. McCormick, T. J. Swissler, M. T. Osborn, M. H. Fuller, and G. K. Yue, *J. geophys. Res.* **94**, 8435 (1989).
33. L. W. Thomason, *Geophys. Res. Lett.* **19**, 2179 (1992).
34. T. Deshler, D. J. Hofmann, B. J. Johnson, and W. R. Rozier, *Geophys. Res. Lett.* **19**, 199 (1992).
35. P. J. Sheridan, R. C. Schnell, D. J. Hoffman, and R. Deshler, *Geophys. Res. Lett.* **19**, 203 (1992).